Bioluminscent *Mycobacterium ulcerans*, a tool to study host-pathogen interactions in a murine tail model of Buruli ulcer

Till F. Omansen[1,2], Renee A. Marcsisin[1], Brendon Y. Chua[1], Weiguang Zeng[1], David C. Jackson[1], Jessica L. Porter[1], Ymkje Stienstra[2], Tjip S. van der Werf[2,3], Timothy P. Stinear[1*]

Affiliations:

[1] Department of Microbiology and Immunology, The Peter Doherty Institute for Infection and Immunity, University of Melbourne, Parkville, VIC 3010, Australia.

[2] University of Groningen, Department of Internal Medicine/Infectious diseases, University Medical Center Groningen, 9700 RB Groningen, The Netherlands.

[3] University of Groningen, Department of Pulmonary Diseases & Tuberculosis, University Medical Center Groningen, 9700 RB Groningen, The Netherlands.

* Corresponding author: Prof. Timothy P. Stinear, Department of Microbiology and Immunology, The Peter Doherty Institute for Infection and Immunity, University of Melbourne, Parkville, VIC 3010, Australia, tstinear@unimelb.edu.au

Running title: **"**Bioluminescent *M. ulcerans* mouse-tail model"

Key words: Buruli ulcer, *Mycobacterium ulcerans*, Bioluminescence, mouse-model, immune response

Abstract

Buruli ulcer is a neglected tropical disease caused by infection with *Mycobacterium ulcerans*. In this study we used a previously reported strain of *M. ulcerans*, genetically engineered to constitutively produce bioluminescence, to follow the progression of Buruli ulcer in mice using an in-vivo imaging (IVIS®) system. We aimed to characterize a mouse tail infection model for pathogenesis, as well as for pre-clinical vaccine and drug development research for Buruli ulcer. Immune parameters, such as antibody titers and cytokine levels, were determined throughout the course of the infection and histology specimens were examined for comparison with human pathology. Nine out of ten (90%) BALB/c mice infected subcutaneously with 10^5 *M. ulcerans* JKD8049 (containing pMV306 hsp16+luxG13) exhibited light emission from the site of infection over the course of the experiment indicating *M. ulcerans* growth *in-vivo*. Five out of ten (50%) animals developed clinical signs of disease. Antibody titers were overall low and their onset was late, as measured by responses to both heterogenous (bacterial whole cell lysate) and single antigen (Hsp18) targets. IFN- γ, and IL-10 are reported to play a vital role in host control of Buruli ulcer and these cytokines were elevated in animals with pathology. For mice with advanced pathology, histology revealed clusters of acid-fast bacilli within subcutaneous tissue 300-400 μm beneath the epidermis of the tail, with macrophage infiltration and granuloma-formation resembling human Buruli ulcer. This study has shown the utility of using bioluminescent *M. ulcerans* and IVIS® in a mouse tail infection model to study Buruli ulcer infection.

Author summary

Buruli ulcer is one of the so called neglected tropical diseases. It is an infectious disease, mainly occurring in West Africa but also in Australia. It manifests as skin lesion and ulcer. Up to date, the way of transmission is inadequately understood. Also, there is no vaccine to protect against the disease. Buruli ulcer is treatable with a course of antibiotics that need to be given for the duration of two months. More laboratory research is needed to elucidate the mechanism of transmission, develop a vaccine and improve and shorten antibiotic therapy. For this, animal (mouse) models of disease are used. The aim of this study was to refine and improve the mouse tail infection model of Buruli ulcer. For this, we used a genetically modified *Mycobacterium ulcerans* strain that emits light. After infection of animals, light emitted from the bacteria was read out with an in-vivo imaging (IVIS) camera. This allowed us to monitor the location of bacteria in the living animal over time without the need to kill the animal. We also measured parameters of the immune system such as antibodies and cytokines as a baseline for future studies into immunology, vaccine development and pathology of Buruli ulcer. We successfully improved and characterized the mouse tail infection model in Buruli ulcer with the use of modern technology using light emitting bacteria and the IVIS camera.

Introduction

Mycobacterium ulcerans causes the neglected tropical disease (NTD) Buruli ulcer (BU) that can manifest as a skin nodule, plaque, edematous lesion or open skin ulcer characterized by yellowish-white necrosis and undermined edges [1]. The disease generally occurs in clustered foci in rural Central and Western Africa but has also gained prominence in specific regions of south east Australia. Currently, 12 countries actively report Buruli ulcer cases and 33 have ever reported cases [2]. Patients with Buruli ulcer suffer from stigmatization, social participation restrictions and physical disability long after even treatment is complete [3]. The main pathogenic factor in BU is a diffusible cytotoxin called mycolactone. Mycolactone is a polyketide-derived macrolide that is responsible for the pathological triad of necrosis, suppressed local inflammatory response and hypoalgesia of the lesion [4,5]. By means of preventing protein translocation into the endoplasmic reticulum, mycolactone suppresses an efficient host innate and adaptive immune response [6,7]. The 174kb large plasmid pMUM001 is responsible for ML production by *M. ulcerans* [8].

There are several major challenges to control Buruli ulcer. The mode of transmission is not yet completely understood and seems to vary by geographic location, although puncturing injuries after contamination from an environmental source seem to be a major cause and in south east Australia at least, mosquitoes have been linked to transmission [9]. Buruli ulcer is currently treated with an eight-week regimen of rifampin and streptomycin or a regimen where the injectable streptomycin is replaced with clarithromycin after four weeks; a fully oral, eight-week rifampin and clarithromycin regimen has been trialled in humans and

88 current trial analysis is ongoing (ClinicalTrials.gov Identifier: NCT01659437) [10,11].
89 Progressed, larger lesions are often managed with surgical excision of the infected tissue
90 followed by functional repair and skin grafting [12]; a recent study showed that the time-
91 point for decision making on whether to intervene surgically or not does not matter for
92 overall healing outcomes [13]. No vaccine is available despite several efforts to employ
93 the BCG-vaccine or to develop novel vaccines [14-23].
94
95 More preclinical research in *M. ulcerans* transmission, chemotherapy and vaccination as
96 well as pathogenesis, is necessary to solve the biomedical challenges complicating Buruli
97 ulcer infection control in the field. In this respect, *M. ulcerans* mouse-infection models
98 have been pivotal in guiding research and clinical studies regarding these questions in the
99 past [24-26]. Murine footpad and tail infection are established methods to study *M.*
100 *ulcerans* [24,27]. The footpad-model has been derived from experience with experimental
101 infection of *M. leprae* in mice [24,28]. It has been used in numerous pre-clinical studies,
102 to mainly evaluate drug efficacy, but also vaccines for *M. ulcerans* [25,26,29-41]. Tail
103 infection has been used to study pathology and vector research [27] and vaccinology [14].
104 Given that Buruli ulcer in humans is a subcutaneous infection mostly occurring on the
105 lower and upper limbs [1,42], the mouse foot and tail are obvious sites to model the disease
106 and the absence of fur in mice allows for easy clinical observation at these sites. Tail
107 infection offers a cutaneous infection site that is not in contact with the environment as
108 much as the footpad so that contamination, re-distribution or loss of inoculum and animal
109 impairment in more advanced stages of the disease are less likely to occur. Also, it is a
110 more practical region for imaging than the footpad. Bioluminescent strains of *M. ulcerans*

111 have successfully been employed to evaluate drug efficacy in *in-vitro* and *in-vivo* drug
112 efficacy studies [36,37,41,43] and in vector ecology studies of *M. ulcerans* [44]. Drug
113 efficacy studies used a luminometer to assess light emission from infected mouse footpads
114 [36,41,45].
115
116 In this study, we aimed to employed the use of a bioluminescent reporter strain of *M.*
117 *ulcerans* to infect BALB/c mice and read out light emission using an in-vivo imaging
118 system (IVIS®) that is both very sensitive at detecting light and enables us to visualize
119 signals from the entire mouse body and thus localize the bacteria. This allows to confirm
120 the site of infection and study possible spread of bacteria. We also characterized the
121 immune-responses to this *M. ulcerans* strain in infected BALB/c mice over a long-term
122 infection period of 17 weeks to establish a baseline for future transmission, vaccine and
123 chemotherapy studies.
124
125 The bioluminescent *M. ulcerans* strain used in this study has been previously described and
126 contains the pMV306 hsp16+luxG13 reporter plasmid [43,46,47] that integrates into the
127 mycobacterial chromosome and contains the lux operon (luxABCDE). Thus, it does not
128 require the addition of an exogenous substrate to detect bioluminescence [46].
129 Bioluminescent infection-models offer the possibility of *in vivo* imaging, with the
130 luminescence read-out serving as proxy for bacterial burden. This approach greatly reduces
131 mouse experiment sample sizes, preventing multiple animals to be killed for a common
132 microbiological assessment such as counting bacterial colony-forming units (CFU) at

different time points. It also offers a way to visualize disease progression over time, as well as bacterial spread in the living host.

Materials and Methods

Culture conditions: *M. ulcerans* JKD8049 harbouring pMV306 hsp16+luxG13 was grown on Middlebrook 7H10 agar or in 7H9 broth containing 10% Oleic Albumin Dextrose Catalase Growth Supplement (Middlebrook, Becton Dickinson, Sparks, MD, USA), 0.5% glycerol and 25μg/ml kanamycin sulfate (Amresco, Solon, OH, USA). Plates and flasks were incubated for 8-10 weeks at 30°C, 5% CO_2. LC-MS was used to confirm that bioluminescent bacteria were still producing mycolactones [48].

Establishing a standard curve for bioluminescent *M. ulcerans* JKD8049. Light emission in photos/sec was compared with colony-forming units (CFU) for *M. ulcerans* JKD8049 cultured in Middlebrook 7H9 medium for 4 weeks and then diluted in serial 10-fold steps in 96-well trays. Photon emissions were captured using a Lumina XRMS Series III In Vitro Imaging System (IVIS®) (Perkin Elmer, Waltham, MA, USA). Bacterial CFUs were confirmed by the spot plate method [9].

Mouse-tail infections: Animal experimentation adhered to the Australian National Health and Medical Research Council Code for the Care and Use of Animals for Scientific Purposes and was approved by and performed in accordance with the University of Melbourne animal ethics committee (Application: 1312756.1). The animals were

purchased from ARC (Canning Vale, Australia). Upon arrival, animals acclimatized for 5 days. Food and water were given *ad libitum*. Ten six-week old, female BALB/c mice were inoculated with approximately 10^5 *M. ulcerans* CFU by subcutaneous (SC) injection into the dorsal aspect of the upper third of the tail. The concentration of the bacterial inocula was confirmed by spot plating. After 17 weeks post-inoculation or whenever the humane endpoint was reached, mice were humanely killed.

***In-vivo* imaging:** Mice were imaged once a week during morning time using a Lumina XRMS Series III IVIS® as described above. During imaging, mice were anaesthetized with 2.5% isofluorane gas (Ceva Animal Health, Glenorie, NSW, Australia) with the stage on which the mice were placed during imaging was warmed to 37°C. Photon emissions were acquired with the following settings: exposure time 5 minutes, emission filter: open, excitation filter: blocked, binning: medium, F/stop 1. These images were superposed onto conventional black/white photographs (exposure time: auto, binning: medium, F/stop: 16). Images from the ventral and dorsal aspect of the tail were taken. Images were analyzed using Living Image® software. Areas emitting light were defined as regions of interest (ROI). A copy of every ROI was placed next to those areas for background measurement. Photons per second from the ROIs were computed and values from control regions subtracted from the actual ROI. Results from ventral and dorsal images (Fig. 1B) were added and the cumulative luminescence of the two imaging angles reported.

ELISA: Blood samples were obtained by sub-mandibular puncture and, at experimental endpoint, by cardiac puncture. Serum was collected by centrifugation and stored at -20°C.

All incubation of ELISA-plates was done in a moisturized container at room temperature. Flat-bottom polyvinyl chloride microtiter-plates (Thermo Fischer, Milford, MA, USA) were coated with 5µg of the antigen overnight. Antigens used were the mycobacterial small heat-shock protein 18 (Hsp18) and *M. ulcerans* whole cell lysate (WCL). The antigen was discarded and plates blocked for 1h with PBS containing 10mg/ml bovine serum albumin (BSA). Plates were washed four times with PBS containing 0.05% Tween-20 (PBST). Sera were added in eight serial dilutions in PBS to the plate and incubated for 4 h. Plates were washed with PBST again and 50µl/well HRP-conjugated polyclonal rabbit anti-mouse Ig-antibody (Dako, Glostrup, Denmark) was added for 1h. Subsequently, ELISA substrate (0.2 mM 2,29-azino-bis 3-ethylbenzthiazoline-sulfonic acid in 50 mM citric acid containing 0.004% hydrogen peroxide) was added to detect bound antibodies. Absorbance was read in a plate reader at 405nm and 450nm and the average of the two wavelengths recorded.

Intracellular cytokine staining and FACS: Dissected spleens were homogenized with a mesh and ATC treated. Splenocytes ($1x10^6$) were re-stimulated with 2µg *M. ulcerans* JKD8049 whole cell lysate (WCL) in RPMI 1640 supplemented with 64mM L-glutamine, 32 mM sodium pyruvate, 1.75mM 2-mercaptoethanol, 3165µg/ml penicillin (all Gibco® Life Technologies, NY, USA), 760 µg/ml gentamicin (G-Bioscience, St. Louis, MO, USA) and 10% heat-inactivated fetal calf serum (CSL, Parkville, Australia) for 72h at 37°C, 5% CO_2. Plates were spun down, supernatant collected and stored at -20°C. Cytokines were stained using the bead-based Cytometric Bead Array (CBA) Mouse Th1/Th2/Th17 Cytokine Kit (BD, North Ryde, NSW, Australia) according to the manufacturer's

202 instructions. Samples were run on a BD FACSCanto™ II Flow Cytometry System and data
203 analyzed using FCAP Array™ Analysis Software version 3.0.
204
205 **Histology:** A section ranging approximately 5mm from the midline of the ulcer proximally
206 was dissected and stored in 10% buffered formalin for histological assessment. Prepared
207 paraffin blocks were surface-decalcified with 10% nitric acid for 5 minutes before cutting
208 4µm sections. Hematoxylin and eosin (HE) and Ziehl-Neelsen (ZN) straining were used
209 following standard protocols. The specimens were subjected for analysis by an independent
210 pathologist. Presence of AFB, inflammatory cells (macrophages, plasma cells/lymphocytes,
211 neutrophils and eosinophils) as well as the degree of inflammation (granulomas,
212 panniculitis, calcification, vasculitis, neuritis) and the tissue damage (dermal and fat tissue
213 necrosis, muscle layer involvement and bone change) and the vascular involvement were
214 scored. Specimens from two non-infected, naïve mice were used as controls.
215
216 **Statistical analysis:** Statistical analysis was performed using GraphPad Prism version 7.0a
217 (GraphPad Software, Inc., San Diego, CA). RLU data were graphed as mean of the ventral
218 and dorsal reading, as described above. Time to bioluminescence is displayed as survival
219 curve. Antibody titers are represented as the reciprocal of the highest dilutions of serum
220 needed to measure an absorbance value of 0.2. This was achieved by transformation of the
221 data by plotting absorbance values vs log0.5—fold dilutions data of each group and using
222 a nonlinear regression analysis of to obtain a line of best fit (with 95% CI) to which the
223 intersect value of 0.2 was determined (Prism 5 or whatever version). One-way ANOVA
224 followed by a Tukey's multiple comparisons test assuming an alpha of 0.05 was used to

test for statistical significant difference between antibody titer measurements. Cytokine readings are shown compared using descriptive statistics.

Results

Standard curve comparing photon/s with CFU readout

To compare bioluminescence read-out with actual bacterial burden, we first established a standard curve *in-vitro*. We applied IVIS® imaging to samples of JKD8049 pMV306 hsp16+luxG13 in different dilutions and plated these on agar for CFU determination. We were able to interpolate a standard curve by nonlinear regression showing a very high positive correlation ($r^2 = 0.98$) between photons/s and CFU/ml (Fig 1A).

Establishment of mouse tail infection.

In order to evaluate virulence and to study murine infection, bioluminescent *M. ulcerans* was injected subcutaneously into mouse tails. Ten BALB/c mice were inoculated with $3.3x10^5$ CFU/ml *M. ulcerans* JKD8049 pMV306 hsp16+luxG13. This resulted in 90% (9 out of 10) of mice presenting measurable light emission on IVIS®-images. Other than at the injection site at the tail, no other foci of infection as indicated by bioluminescence were observed (Fig 1B). Fifty percent (5 out of 10) gradually developed macroscopically apparent lesions resembling Buruli ulcer within 17 weeks (Fig 1C). None of the animals showed other signs of illness than skin lesion that were restricted to the approximate sites of injection.

248 **Course of the infection as measured by bioluminescence**

249 To study the course of the infection in terms of bacterial burden measured in
250 bioluminescence, mice were imaged weekly with the IVIS® system. Bioluminescence,
251 measured in emitted photons/s rose exponentially to a maximum of $1x10^7$ in week seven
252 (Fig 1D), according to our standard curve, this equals about $5x10^6$ CFU/ml (Fig 1A) and
253 was associated with advanced, severe pathology (Table 1). From this time-point on, the
254 signal declined to a $1x10^5$ (corresponding to $4x10^4$ bacteria) threshold until the end of the
255 experiment. At week eight, three mice reached humane endpoint and were culled. In
256 examining the antibody titer levels against MU WCL, these began to rise in week 8,
257 correlating with a decrease in photon/s counts. Animals displaying *severe* symptoms had
258 higher photons/s counts, indicating higher bacterial burden, compared to those with
259 *moderate* or no pathology. Photons/sec counts increased per week until week 6-8 when the
260 infection seemed to plateau.

261

262 **Table 1: Overview of histopathological findings of mice subcutaneously infected with**
263 **autoluminescent *M. ulcerans* into the tail.** Animals were divided by clinical pathology in
264 severe pathology, moderate pathology and no marcopathology. Photons per second
265 analyzed by IVIS-imaging are shown in comparison to histological results. The amount of
266 photos/s as a proxy for bacterial quantity correlated with pathology except in mouse 87,
267 where no clinical pathology was seen.

Clinical picture	ID	BL-AUC	AFB	INF	TDM	VAS	Inflammatory cell type	Degree of inflammation
Severe pathology (sacrificed at week 8)	84	1.36 E+08	++	+++	+++	n/a	PC, MΦ, LYM	Severe, multifocal, chronic
	85	1.35 E+08	+++	+++	+++	n/a	PC, MΦ, LYM, EOS	Severe, multifocal, chronic
	88	1.72 E+07	++	+++	+++	++	PC, MΦ, LYM	Severe, multifocal, chronic

Moderate pathology	86	1.97 E+06	-	+	+	+	MΦ, LYM	Mild to moderate, chronic, multifocal
	89	3.69 E+06	+	+/++	++	++	PC, MΦ	Mild, diffuse, chronic
No macro pathology	81	2.15 E+06	-	+	+	-	MΦ, LYM	Moderate, chronic, focal
	82	692641	-	-	-	-	-	None
	83	872438	-	+	+	+	MΦ, LYM	Moderate, chronic, multifocal
	87	7.24 E+06	++	+++	+++	++	PC, MΦ, LYM	Locally severe, chronic
	90	0	-	+	+	+	PC, MΦ, EOS, NEU	Mild, chronic, multifocal

ID, Identifier; BL-AUC, Bioluminescence in photons/s Area under the Curve; AFB, acid-fast bacilli, INF, inflammation; TDM, tissue damage; VAS, vascular involvement; PC, Plasma cell; MΦ, Macrophage, LYM, lymphocyte; EOS, eosinophil; NEU, neutrophil.

Antibody titers

To characterize the antibody-mediated immune response to *M. ulcerans*, we obtained plasma samples for ELISA at weeks 2, 4, 7, 13 and 17 of the experiment. Over time, there was a slight increase of antibody titers in response to *M. ulcerans* WCL but overall a late onset of the antibody response was noted (Fig 2A). Antibody titers reached higher levels between week 11 and 17, but overall titers, were low (Fig 2A). The response to *M. ulcerans* Hsp18 and WCL was compared and no statistically significant difference ($p > 0.05$) was found (Fig 2B). Furthermore, ELISA results in response to WCL at week 8 were compared between animals with severe, moderate and no clinical pathology and no statistically significant difference ($p > 0.05$) was found (Fig 2C,D).

Late suppression of cytokines

To characterize and study the cytokine profile in our murine *M. ulcerans* infection model, intracellular cytokine staining was performed on spleen samples after eight and 17 weeks

of the experiment, when three mice were humanely killed. The cytokine concentrations in splenocyte samples re-stimulated with 2µg *M. ulcerans* JKD8049 WCL were compared between mice with pathology culled at week 8 and those with and without pathology culled at week 17 were compared. In the three mice that were culled prematurely due to rapidly extending disease in week 8, elevated levels of IFN-γ and IL-10 were measured. Overall, cytokine levels were very low for all assayed cytokines in week 17 regardless of clinical state of the animal (Fig 3).

Histopathology of lesions

In order to validate the model and study the pathology of *M. ulcerans,* histopathology was performed on skin lesions and compared to those of humans described in the literature. Specimens from infected tissue were subjected to histopathological analysis in Ziehl-Neelsen and H&E-staining. Aggregates of acid-fast bacilli, *M. ulcerans*, were observed at 300 – 400 µm beneath the epidermis (Fig 4A). Furthermore, epidermal hyperplasia and immune cell infiltrates were apparent (Fig. 4). Bioluminescence (photons/s) as proxy for bacterial quantity correlated well with the histological extent of disease except for mouse ID 87 (Table 1). Numerous acid-fast bacilli as well as severe, multifocal, chronic inflammation marked by presence of plasma cells, macrophages and lymphocytes were observed in mice with severe clinical pathology. There was extensive tissue damage, as well as vascular involvement in these animals. Mice with moderate clinical pathology exhibited mild and rather diffuse histological pictures and less tissue damage. Mice that had no obvious clinical signs of disease had low bioluminescence and showed moderate to little localized/focal histological features of inflammation (Table 1, Fig 4).

309

310 **Discussion**

311 In this study we have successfully applied the use of bioluminescent *M. ulcerans* JKD8049
312 to develop a model that allows us to follow the immune response to *M. ulcerans* in BALB/c
313 mice correlating with human Buruli ulcer disease. The onset of clinical signs was gradual
314 and mice developed characteristic, localized lesions. Necrosis of the subcutis, chronic
315 inflammation with the presence of macrophages and lymphocytes, granuloma formation,
316 panniculitis as well as the and presence of AFBs correlating with disease progression are
317 hallmarks of Buruli ulcer histopathology described in humans [49,50]. The extent and the
318 overall of pathology observed in the mouse tail tissue in our study was comparable to the
319 above-mentioned experience from human patients supporting the use of this mouse model
320 to study Buruli ulcer.

321

322 The bioluminescent read-out correlated with the histopathological outcome in a dose-
323 dependent manner, where an elevated photons/s counts, indicating high bacterial burden
324 coincided with more progressive histological disease (Table 1) underlining the usefulness
325 of IVIS®-imaging and bioluminescence as a marker for disease progression. The use of
326 bioluminescent *M. ulcerans* permitted us to both verify the location of the bacteria as well
327 as the growth rate in the lesion. After subcutaneous injection we observed presence of
328 photon-emitting bacteria exclusively in the upper-third of the mouse tail, which was the
329 site of injection.

330

We noticed a decline and plateauing of bioluminescence from week 8 onwards. This phenomenon could be explained by a plateauing of the bacterial growth curve in the lesion and transition into a stationary phase where less of the immunosuppressive toxin mycolactone is produced and partial host control sets in which is reflected to some extent by the rise of antibody titers around that time-point (Fig 2). The later phase of Buruli ulcer infection is characterized by granuloma formation and highly localized extracellular AFBs within these lesions. Also, a less active metabolic state during this phase could lead to decreased bioluminescence. Vasculopathy is a feature of Buruli ulcers observed in humans [49] and mice (Table 1, Fig 4). A hypoxic state within the lesion might also decrease bioluminescence and more research is needed to elucidate the usefulness of bioluminescence as a marker of bacterial quantity beyond approx. 8 weeks of infection in the BALB/c mouse.

Immunology and course of disease

The immune response to *M. ulcerans* is influenced by the microbes' toxin, mycolactone. Dendritic cells (DC's) are inhibited by ML which can impair their ability to prime a cellular immune responses and phagocytose the bacteria [51]. Also, suppression of a CD4+ immune response was observed in humans [52,53] and efficient mounting of a Th1 response and elevated IFN-γ seemed protective [54]. T-cells depletion, mediated by miRNAs has also been attributed to ML {GueninMace:2011bp}. It is believed that, like in tuberculosis, an effective cell-mediated immune responses can naturally control the infection a nd are likely also important for conferring transient protection against BU, experimentally [55]. Markedly elevated cytokines in human Buruli cases are IFN-γ and

354 IL-10 [56]. IFN-γ is known to be an early mediator of host response to *M. ulcerans* [57]
355 and increases in patients after 4 – 8 weeks of antimicrobial treatment indicating
356 immunocompetence against *M. ulcerans* and the mounting of a supportive CD4+ Th1-
357 response [56]. The elevated IFN-γ response seen in mice with severe pathology (Fig 3A)
358 can thus be interpreted as an early reaction to a large amount of actively multiplying
359 bacteria, whereas at week 17, mice with no pathology had higher IFN-γ levels than those
360 with pathology possibly due to sufficient host control of the pathogen. Consistently,
361 patients with pre-ulcerative lesions (early-phase) and patients with healed lesions (host
362 control) both showed elevated IFN-γ levels [58] whilst IL-10 seems to be somewhat
363 nonspecifically elevated during all phases of Buruli ulcer disease [54,56,58]
364
365 In our experiment, we noted a late onset of cell-mediated immunity in the mice infected
366 with *M. ulcerans.* Antibody titres slowly rose, but only at week 7. Interestingly, the decline
367 in photons/s and the increase in antibody titers coincided in week 7. It is not clear if rising
368 antibody levels helped to gain control of the infection or if declining bacterial load resulted
369 in less immune suppression by ML and led to a reactivation of the immune system and an
370 increase of antibody levels. In humans, serological screening for Hsp18 antibodies
371 indicates that large parts of the population in endemic areas are exposed to *M. ulcerans* but
372 only some develop the disease [59]. Guinea pigs infected with *M. ulcerans* appear to self-
373 heal as do some mice [60]. It is conceivable that humans infected with certain doses of *M.*
374 *ulcerans* develop either no disease, limited disease, or even unnoticed disease that self-
375 resolves. Evidence for these scenarios has been observed in Buruli ulcer patients who have
376 defaulted from antibiotic treatment regimens, yet could still be contacted for follow-up and

377 showed to have healed lesions despite incomplete treatment [61]. It is likely, that the
378 bacterial burden was not zero in these patients at the time of default but that it reached a
379 critical nadir at which host immunity overcame the counteracting effect of mycolactone
380 and controlled infection. Individuals that are able to establish an efficient immune response
381 to MU might control and clear the infection unnoticed as was the case with 50% of
382 subcutaneously infected mice in our experiment. We have previously deduced a low
383 infectious dose 50% (ID50) of <10 CFU from experiments involving mechanical injury
384 simulated by needle stick to *M. ulcerans* externally contaminated mouse tails. Even though
385 in this current research bacterial presence was measured by IVIS® imaging in 90% of mice,
386 only 50% of animals showed clinical disease in this experiment following subcutaneous
387 injection with approx. $5x10^6$ CFU/ml. This observation and discrepancy with our previous
388 research might be explained by the different handling of the inoculating needle,
389 perpendicular, and supposedly deeper penetration in the study by Wallace et al. [9] and
390 more superficial penetration in a 20-30° angle in subcutaneous injections in this study.
391 Experiments are required to assess the *M. ulcerans* ID50 using carefully controlled
392 inoculation conditions, perhaps using a micromanipulator with decreasing doses of *M.*
393 *ulcerans*.
394
395 At week 8, three animals of the SC cohort had reached the humane experimental endpoint
396 and were culled. Their cytokine profile data were comparable to those of the other animals
397 culled at week 17 and provide an insight into the evolution of the cytokine profile. While
398 there were considerable amounts of IFN-γ and IL-10 indicating a Th1-mediated response
399 observed in the animals sacrificed at week 8, all cytokine levels were reduced by week 17.

The suppression of cytokines is due to inhibition by ML of nascent membrane and secretory proteins egress through the ER membrane [6,62]. In human patients with Buruli ulcer, overall suppressed IFN-γ levels are seen [54]. The triad of peak bacterial load with worsening pathology, low but rising antibody titers and elevated Th1 subset cytokines in week 7 could also explain the paradoxical response seen in patients; an overreaction and inflammation of the reactivating immune system noted in patients beginning antibiotics for Buruli ulcer [63]. Animals not showing clinical signs of disease had marginally higher antibodies levels against *M. ulcerans* (Fig 2) possibly indicating some sort of immune response to the infection, though the results were statistically not significant in our small sample.

We demonstrated virulence of the *M. ulcerans*+pMV306 hsp16+luxG13 reporter strain and observed localized clinical disease with human-like pathology in 50% of the animals after inoculation with $5x10^6$ CFU/ml bacteria. IVIS®-imaging of *M. ulcerans* infection can reduce and refine animal usage in Buruli ulcer research and enables further studies of into pathology of the disease as well as pre-clinical drug and vaccine evaluation.

Acknowledgements

We thank Rolfe Howlett and John Hayman and for help with analyzing and scoring the histopathological results.

421 **References**

422

423 1. van der Werf TS, Stienstra Y, Johnson RC, Phillips R, Adjei O, Fleischer B, et al.
424 Mycobacterium ulcerans disease. Bull World Health Organ. 2005;83: 785–791.
425 2. WHO. Buruli ulcer [Internet].
426 3. de Zeeuw J, Omansen TF, Douwstra M, Barogui YT, Agossadou C, Sopoh GE, et
427 al. Persisting social participation restrictions among former Buruli ulcer patients in
428 Ghana and Benin. Small PLC, editor. PLoS Negl Trop Dis. Public Library of
429 Science; 2014;8: e3303. doi:10.1371/journal.pntd.0003303
430 4. George KM, Chatterjee D, Gunawardana G, Welty D, Hayman J, Lee R, et al.
431 Mycolactone: a polyketide toxin from Mycobacterium ulcerans required for
432 virulence. Science. 1999;283: 854–857.
433 5. George KM, Pascopella L, Welty DM, Small PL. A Mycobacterium ulcerans
434 toxin, mycolactone, causes apoptosis in guinea pig ulcers and tissue culture cells.
435 Infect Immun. 2000;68: 877–883.
436 6. Hall BS, Hill K, McKenna M, Ogbechi J, High S, Willis AE, et al. The pathogenic
437 mechanism of the Mycobacterium ulcerans virulence factor, mycolactone, depends
438 on blockade of protein translocation into the ER. Deretic V, editor. PLoS Pathog.
439 2014;10: e1004061. doi:10.1371/journal.ppat.1004061
440 7. Demangel C, High S. Sec61 blockade by mycolactone: a central mechanism in
441 Buruli ulcer disease. Biol Cell. 2018. doi:10.1111/boc.201800030
442 8. Stinear TP, Mve-Obiang A, Small PLC, Frigui W, Pryor MJ, Brosch R, et al. Giant
443 plasmid-encoded polyketide synthases produce the macrolide toxin of

444 Mycobacterium ulcerans. Proc Natl Acad Sci USA. 2004;101: 1345–1349.
445 doi:10.1073/pnas.0305877101
446 9. Wallace JR, Mangas KM, Porter JL, Marcsisin R, Pidot SJ, Howden BO, et al.
447 Mycobacterium ulcerans low infectious dose and atypical mechanical transmission
448 support insect bites and puncturing injuries in the spread of Buruli ulcer. bioRxiv.
449 Cold Spring Harbor Labs Journals; 2016;: 071753. doi:10.1101/071753
450 10. Etuaful S, Carbonnelle B, Grosset J, Lucas S, Horsfield C, Phillips R, et al.
451 Efficacy of the combination rifampin-streptomycin in preventing growth of
452 Mycobacterium ulcerans in early lesions of Buruli ulcer in humans. Antimicrob
453 Agents Chemother. American Society for Microbiology; 2005;49: 3182–3186.
454 doi:10.1128/AAC.49.8.3182-3186.2005
455 11. Nienhuis WA, Stienstra Y, Thompson WA, Awuah PC, Abass KM, Tuah W, et al.
456 Antimicrobial treatment for early, limited Mycobacterium ulcerans infection: a
457 randomised controlled trial. Lancet. 2010;375: 664–672. doi:10.1016/S0140-
458 6736(09)61962-0
459 12. Kibadi K, Boelaert M, Fraga AG, Kayinua M, Longatto-Filho A, Minuku J-B, et
460 al. Response to treatment in a prospective cohort of patients with large ulcerated
461 lesions suspected to be Buruli Ulcer (Mycobacterium ulcerans disease). Phillips
462 RO, editor. PLoS Negl Trop Dis. 2010;4: e736. doi:10.1371/journal.pntd.0000736
463 13. Wadagni AC, Barogui YT, Johnson RC, Sopoh GE, Affolabi D, van der Werf TS,
464 et al. Delayed versus standard assessment for excision surgery in patients with
465 Buruli ulcer in Benin: a randomised controlled trial. Lancet Infect Dis. 2018;18:
466 650–656. doi:10.1016/S1473-3099(18)30160-9

14. Coutanceau E, Legras P, Marsollier L, Reysset G, Cole ST, Demangel C. Immunogenicity of Mycobacterium ulcerans Hsp65 and protective efficacy of a Mycobacterium leprae Hsp65-based DNA vaccine against Buruli ulcer. Microbes Infect. 2006;8: 2075–2081. doi:10.1016/j.micinf.2006.03.009

15. Watanabe M, Nakamura H, Nabekura R, Shinoda N, Suzuki E, Saito H. Protective effect of a dewaxed whole-cell vaccine against Mycobacterium ulcerans infection in mice. Vaccine. 2015;33: 2232–2239. doi:10.1016/j.vaccine.2015.03.046

16. Bolz M, Kerber S, Zimmer G, Pluschke G. Use of Recombinant Virus Replicon Particles for Vaccination against Mycobacterium ulcerans Disease. Johnson C, editor. PLoS Negl Trop Dis. 2015;9: e0004011. doi:10.1371/journal.pntd.0004011

17. Hart BE, Hale LP, Lee S. Recombinant BCG Expressing Mycobacterium ulcerans Ag85A Imparts Enhanced Protection against Experimental Buruli ulcer. Johnson C, editor. PLoS Negl Trop Dis. 2015;9: e0004046. doi:10.1371/journal.pntd.0004046

18. Bolz M, Bénard A, Dreyer AM, Kerber S, Vettiger A, Oehlmann W, et al. Vaccination with the Surface Proteins MUL_2232 and MUL_3720 of Mycobacterium ulcerans Induces Antibodies but Fails to Provide Protection against Buruli Ulcer. Small PLC, editor. PLoS Negl Trop Dis. 2016;10: e0004431. doi:10.1371/journal.pntd.0004431

19. Bénard A, Sala C, Pluschke G. Mycobacterium ulcerans Mouse Model Refinement for Pre-Clinical Profiling of Vaccine Candidates. Cardona P-J, editor. PLoS ONE. 2016;11: e0167059. doi:10.1371/journal.pone.0167059

20. Hart BE, Lee S. Overexpression of a Mycobacterium ulcerans Ag85B-EsxH

Fusion Protein in Recombinant BCG Improves Experimental Buruli Ulcer Vaccine Efficacy. Pluschke G, editor. PLoS Negl Trop Dis. 2016;10: e0005229. doi:10.1371/journal.pntd.0005229

21. Smith PG, Revill WD, Lukwago E, Rykushin YP. The protective effect of BCG against Mycobacterium ulcerans disease: a controlled trial in an endemic area of Uganda. Trans R Soc Trop Med Hyg. 1976;70: 449–457.

22. BCG vaccination against mycobacterium ulcerans infection (Buruli ulcer). First results of a trial in Uganda. Lancet. 1969;1: 111–115.

23. Einarsdottir T, Huygen K. Buruli ulcer. Hum Vaccin. 2011;7: 1198–1203. doi:10.4161/hv.7.11.17751

24. Dega H, Robert J, Bonnafous P, Jarlier V, Grosset J. Activities of several antimicrobials against Mycobacterium ulcerans infection in mice. Antimicrob Agents Chemother. American Society for Microbiology (ASM); 2000;44: 2367–2372.

25. Bentoucha A, Robert J, Dega H, Lounis N, Jarlier V, Grosset J. Activities of new macrolides and fluoroquinolones against Mycobacterium ulcerans infection in mice. Antimicrob Agents Chemother. American Society for Microbiology; 2001;45: 3109–3112. doi:10.1128/AAC.45.11.3109-3112.2001

26. Dega H, Bentoucha A, Robert J, Jarlier V, Grosset J. Bactericidal activity of rifampin-amikacin against Mycobacterium ulcerans in mice. Antimicrob Agents Chemother. American Society for Microbiology (ASM); 2002;46: 3193–3196. doi:10.1128/AAC.46.10.3193-3196.2002

27. Marsollier L, Robert R, Aubry J, Saint André J-P, Kouakou H, Legras P, et al.

513 Aquatic insects as a vector for Mycobacterium ulcerans. Appl Environ Microbiol.
514 2002;68: 4623–4628.
515 28. Shepard CC. THE EXPERIMENTAL DISEASE THAT FOLLOWS THE
516 INJECTION OF HUMAN LEPROSY BACILLI INTO FOOT-PADS OF MICE. J
517 Exp Med. 1960;112: 445–454.
518 29. Tanghe A, Dangy J-P, Pluschke G, Huygen K. Improved protective efficacy of a
519 species-specific DNA vaccine encoding mycolyl-transferase Ag85A from
520 Mycobacterium ulcerans by homologous protein boosting. Small PLC, editor.
521 PLoS Negl Trop Dis. 2008;2: e199. doi:10.1371/journal.pntd.0000199
522 30. Tanghe A, Adnet P-Y, Gartner T, Huygen K. A booster vaccination with
523 Mycobacterium bovis BCG does not increase the protective effect of the vaccine
524 against experimental Mycobacterium ulcerans infection in mice. Infect Immun.
525 2007;75: 2642–2644. doi:10.1128/IAI.01622-06
526 31. Dhople AM, Namba K. Activities of sitafloxacin (DU-6859a), either singly or in
527 combination with rifampin, against Mycobacterium ulcerans infection in mice. J
528 Chemother. 2003;15: 47–52. doi:10.1179/joc.2003.15.1.47
529 32. Converse PJ, Almeida DV, Tasneen R, Saini V, Tyagi S, Ammerman NC, et al.
530 Shorter-course treatment for Mycobacterium ulcerans disease with high-dose
531 rifamycins and clofazimine in a mouse model of Buruli ulcer. Small PLC, editor.
532 PLoS Negl Trop Dis. 2018;12: e0006728. doi:10.1371/journal.pntd.0006728
533 33. Converse PJ, Xing Y, Kim KH, Tyagi S, Li S-Y, Almeida DV, et al. Accelerated
534 detection of mycolactone production and response to antibiotic treatment in a
535 mouse model of Mycobacterium ulcerans disease. Phillips RO, editor. PLoS Negl

536 Trop Dis. 2014;8: e2618. doi:10.1371/journal.pntd.0002618

537 34. Sarfo FS, Converse PJ, Almeida DV, Zhang J, Robinson C, Wansbrough-Jones M,
538 et al. Microbiological, histological, immunological, and toxin response to
539 antibiotic treatment in the mouse model of Mycobacterium ulcerans disease. Small
540 PLC, editor. PLoS Negl Trop Dis. 2013;7: e2101.
541 doi:10.1371/journal.pntd.0002101

542 35. Converse PJ, Almeida DV, Nuermberger EL, Grosset JH. BCG-mediated
543 protection against Mycobacterium ulcerans infection in the mouse. Roy CR, editor.
544 PLoS Negl Trop Dis. 2011;5: e985. doi:10.1371/journal.pntd.0000985

545 36. Zhang T, Li S-Y, Converse PJ, Almeida DV, Grosset JH, Nuermberger EL. Using
546 bioluminescence to monitor treatment response in real time in mice with
547 Mycobacterium ulcerans infection. Antimicrob Agents Chemother. 2011;55: 56–
548 61. doi:10.1128/AAC.01260-10

549 37. Zhang T, Bishai WR, Grosset JH, Nuermberger EL. Rapid assessment of
550 antibacterial activity against Mycobacterium ulcerans by using recombinant
551 luminescent strains. Antimicrob Agents Chemother. 2010;54: 2806–2813.
552 doi:10.1128/AAC.00400-10

553 38. Almeida D, Converse PJ, Ahmad Z, Dooley KE, Nuermberger EL, Grosset JH.
554 Activities of rifampin, Rifapentine and clarithromycin alone and in combination
555 against mycobacterium ulcerans disease in mice. Diemert DJ, editor. PLoS Negl
556 Trop Dis. 2011;5: e933. doi:10.1371/journal.pntd.0000933

557 39. Almeida DV, Converse PJ, Li S-Y, Tyagi S, Nuermberger EL, Grosset JH.
558 Bactericidal activity does not predict sterilizing activity: the case of rifapentine in

559 the murine model of Mycobacterium ulcerans disease. Johnson C, editor. PLoS
560 Negl Trop Dis. 2013;7: e2085. doi:10.1371/journal.pntd.0002085
561 40. Converse PJ, Tyagi S, Xing Y, Li S-Y, Kishi Y, Adamson J, et al. Efficacy of
562 Rifampin Plus Clofazimine in a Murine Model of Mycobacterium ulcerans
563 Disease. Phillips RO, editor. PLoS Negl Trop Dis. 2015;9: e0003823.
564 doi:10.1371/journal.pntd.0003823
565 41. Zhang T, Li S-Y, Converse PJ, Grosset JH, Nuermberger EL. Rapid, serial, non-
566 invasive assessment of drug efficacy in mice with autoluminescent Mycobacterium
567 ulcerans infection. Ricaldi JN, editor. PLoS Negl Trop Dis. 2013;7: e2598.
568 doi:10.1371/journal.pntd.0002598
569 42. Yerramilli A, Tay EL, Stewardson AJ, Kelley PG, Bishop E, Jenkin GA, et al. The
570 location of Australian Buruli ulcer lesions-Implications for unravelling disease
571 transmission. Pluschke G, editor. PLoS Negl Trop Dis. 2017;11: e0005800.
572 doi:10.1371/journal.pntd.0005800
573 43. Omansen TF, Porter JL, Johnson PDR, van der Werf TS, Stienstra Y, Stinear TP.
574 In-vitro activity of avermectins against Mycobacterium ulcerans. Johnson C,
575 editor. PLoS Negl Trop Dis. Public Library of Science; 2015;9: e0003549.
576 doi:10.1371/journal.pntd.0003549
577 44. Wallace JR, Mangas KM, Porter JL, Marcsisin R, Pidot SJ, Howden B, et al.
578 Mycobacterium ulcerans low infectious dose and mechanical transmission support
579 insect bites and puncturing injuries in the spread of Buruli ulcer. Azman AS,
580 editor. PLoS Negl Trop Dis. 2017;11: e0005553.
581 doi:10.1371/journal.pntd.0005553

582 45. Zhang T, Li S-Y, Nuermberger EL. Autoluminescent Mycobacterium tuberculosis
583 for rapid, real-time, non-invasive assessment of drug and vaccine efficacy. Tyagi
584 AK, editor. PLoS ONE. 2012;7: e29774. doi:10.1371/journal.pone.0029774
585 46. Andreu N, Zelmer A, Fletcher T, Elkington PT, Ward TH, Ripoll J, et al.
586 Optimisation of bioluminescent reporters for use with mycobacteria. Doherty TM,
587 editor. PLoS ONE. 2010;5: e10777. doi:10.1371/journal.pone.0010777
588 47. Andreu N, Zelmer A, Sampson SL, Ikeh M, Bancroft GJ, Schaible UE, et al. Rapid
589 in vivo assessment of drug efficacy against Mycobacterium tuberculosis using an
590 improved firefly luciferase. J Antimicrob Chemother. 2013;68: 2118–2127.
591 doi:10.1093/jac/dkt155
592 48. Hong H, Gates PJ, Staunton J, Stinear T, Cole ST, Leadlay PF, et al. Identification
593 using LC-MSn of co-metabolites in the biosynthesis of the polyketide toxin
594 mycolactone by a clinical isolate of Mycobacterium ulcerans. Chem Commun
595 (Camb). 2003;: 2822–2823.
596 49. Guarner J, Bartlett J, Whitney EAS, Raghunathan PL, Stienstra Y, Asamoa K, et
597 al. Histopathologic features of Mycobacterium ulcerans infection. Emerging Infect
598 Dis. 2003;9: 651–656.
599 50. Rondini S, Horsfield C, Mensah-Quainoo E, Junghanss T, Lucas S, Pluschke G.
600 Contiguous spread of Mycobacterium ulcerans in Buruli ulcer lesions analysed by
601 histopathology and real-time PCR quantification of mycobacterial DNA. J Pathol.
602 2006;208: 119–128. doi:10.1002/path.1864
603 51. Coutanceau E, Decalf J, Martino A, Babon A, Winter N, Cole ST, et al. Selective
604 suppression of dendritic cell functions by Mycobacterium ulcerans toxin

mycolactone. J Exp Med. 2007;204: 1395–1403. doi:10.1084/jem.20070234

52. Phillips R, Sarfo FS, Guenin-Macé L, Decalf J, Wansbrough-Jones M, Albert ML, et al. Immunosuppressive signature of cutaneous Mycobacterium ulcerans infection in the peripheral blood of patients with buruli ulcer disease. J Infect Dis. 2009;200: 1675–1684. doi:10.1086/646615

53. Boulkroun S, Guenin-Macé L, Thoulouze M-I, Monot M, Merckx A, Langsley G, et al. Mycolactone suppresses T cell responsiveness by altering both early signaling and posttranslational events. J Immunol. 2010;184: 1436–1444. doi:10.4049/jimmunol.0902854

54. Gooding TM, Johnson PDR, Smith M, Kemp AS, Robins-Browne RM. Cytokine profiles of patients infected with Mycobacterium ulcerans and unaffected household contacts. Infect Immun. 2002;70: 5562–5567.

55. Fraga AG, Martins TG, Torrado E, Huygen K, Portaels F, Silva MT, et al. Cellular immunity confers transient protection in experimental Buruli ulcer following BCG or mycolactone-negative Mycobacterium ulcerans vaccination. Manganelli R, editor. PLoS ONE. 2012;7: e33406. doi:10.1371/journal.pone.0033406

56. Sarfo FS, Phillips RO, Ampadu E, Sarpong F, Adentwe E, Wansbrough-Jones M. Dynamics of the cytokine response to Mycobacterium ulcerans during antibiotic treatment for M. ulcerans disease (Buruli ulcer) in humans. Clin Vaccine Immunol. 2009;16: 61–65. doi:10.1128/CVI.00235-08

57. Bieri R, Bolz M, Ruf M-T, Pluschke G. Interferon-γ Is a Crucial Activator of Early Host Immune Defense against Mycobacterium ulcerans Infection in Mice. Johnson C, editor. PLoS Negl Trop Dis. 2016;10: e0004450.

628 doi:10.1371/journal.pntd.0004450

629 58. Schipper HS, Rutgers B, Huitema MG, Etuaful SN, Westenbrink BD, Limburg PC,
630 et al. Systemic and local interferon-gamma production following Mycobacterium
631 ulcerans infection. Clin Exp Immunol. 2007;150: 451–459. doi:10.1111/j.1365-
632 2249.2007.03506.x

633 59. Diaz D, Döbeli H, Yeboah-Manu D, Mensah-Quainoo E, Friedlein A, Soder N, et
634 al. Use of the immunodominant 18-kiloDalton small heat shock protein as a
635 serological marker for exposure to Mycobacterium ulcerans. Clin Vaccine
636 Immunol. 2006;13: 1314–1321. doi:10.1128/CVI.00254-06

637 60. Silva-Gomes R, Marcq E, Trigo G, Gonçalves CM, Longatto-Filho A, Castro AG,
638 et al. Spontaneous Healing of Mycobacterium ulcerans Lesions in the Guinea Pig
639 Model. Johnson C, editor. PLoS Negl Trop Dis. 2015;9: e0004265.
640 doi:10.1371/journal.pntd.0004265

641 61. Klis S, Kingma RA, Tuah W, van der Werf TS, Stienstra Y. Clinical outcomes of
642 Ghanaian Buruli ulcer patients who defaulted from antimicrobial therapy. Trop
643 Med Int Health. 2016;21: 1191–1196. doi:10.1111/tmi.12745

644 62. Simmonds RE, Lali FV, Smallie T, Small PLC, Foxwell BM. Mycolactone inhibits
645 monocyte cytokine production by a posttranscriptional mechanism. J Immunol.
646 2009;182: 2194–2202. doi:10.4049/jimmunol.0802294

647 63. Nienhuis WA, Stienstra Y, Abass KM, Tuah W, Thompson WA, Awuah PC, et al.
648 Paradoxical responses after start of antimicrobial treatment in Mycobacterium
649 ulcerans infection. Clin Infect Dis. 2012;54: 519–526. doi:10.1093/cid/cir856

650

651 **Figure legends**

652 **Figure 1. Use of bioluminescent *M. ulcerans* to follow the evolution of disease in the**
653 **mouse tail model of Buruli ulcer.** (A) Standard curve comparing bioluminescence and
654 colony-forming units (CFU) of the *M. ulcerans* JKD8049 +pMV306 hsp16 luxG13
655 reporter strain. (B) IVIS®- (left) and photographic images (right) from BALB/c mice
656 infected via subcutaneous tail inoculation with approx. $3.3x10^5$ CFU/ml *M. ulcerans*
657 harboring the bioluminescent reporter plasmid. Photons/s emitted from bioluminescent
658 bacteria were detected by IVIS® in anesthetized mice. Results are represented in a pseudo-
659 colored scheme (red indicated high, yellow medium and green low intensity of light
660 emitted). Light was detected from both the dorsal (site of injection) and ventral aspects of
661 the mouse tail. The photos were taken at 4 weeks post infection; the bioluminescence read-
662 out was $1.8x10^6$ photons, corresponding to approx. $6.7x10^5$ CFU/ml according to our
663 standard curve. (C) Survival-graph representing time to detectable bioluminescence
664 emission from mice infected with bioluminescent *M. ulcerans* into the tail (D)
665 Development of mean photons/s emitted from mice infected with $3.3x10^5$ bioluminescent
666 *M. ulcerans* into the upper third of the dorsal tail. Values represent the mean of dorsal and
667 ventral photons/s measurement. Animals were sub-grouped for analysis by clinical staging
668 based on severity of the gross pathology (*severe*: redness, swelling, edema, impending
669 ulceration; *moderate*: redness, edema; and no pathology.
670
671 **Figure 2. Evolution of the antibody titer against *M. ulcerans* whole cell lysate (WCL)**
672 **and small heat shock protein 18 (Hsp18) measured in plasma from mice infected with**
673 ***M. ulcerans* over time.** A late onset of overall antibody response against an unspecific *M.*

674 *ulcerans* whole cell lysate was noted in the bioluminescent *M. ulcerans* tail infection model.
675 Antibody titers rose late, after 8 weeks and plateaued at week 13 (A). No difference ($p > 0.5$)
676 was observed in the antibody titer against small heat-shock protein 18 (Hsp 18) and
677 whole cell lysate (B). No statistically significance in antibody levels was seen between
678 animals with severe, moderate or no apparent pathology ($p > 0.5$; C).
679
680 **Figure 3: Comparison of cytokine profile assessed by intracellular cytokine staining**
681 **(ICS) of mice infected with *M. ulcerans* after 8 (A) and 17 (B) weeks of infection to**
682 **naïve, non-infected mice.** Error bars represent standard error of the mean. Mice with
683 advanced clinical pathology sacrificed at week eight of the experiment displayed highly
684 elevated IFN-γ, as well as IL-6 and IL-10 levels (A). IFN-γ is known to activate
685 macrophages and is a key regulator in granuloma formation in mycobacterial infections.
686 At week 17, infected mice with no apparent pathology had higher IFN-γ counts than other
687 mice, as well as slightly elevated IL-2 levels.
688
689 **Figure 4: Histological specimens of mice infected with *M. ulcerans* into the tail in**
690 **Hematoxylin and Eosin (H&E; A1,B1,C1,D1) or Ziel-Neelsen (ZN; A2,B2, C2,D2)**
691 **staining. (**A) Whole slide cross-section of mouse tail (ID #85) infected with *M. ulcerans*
692 subcutaneously, humanely killed eight weeks' post-infection due to advanced clinical
693 pathology. Visible, are clusters of acid-fast bacilli and in the cutis and subcutis, approx.
694 300-400 µm beneath the surface. (B.1 and B.2) Example of presence of AFB in mouse #
695 85, as well as granuloma formation. (C.1 and C2.) Normal mouse tail histology of a naïve,
696 uninfected mouse with thin epidermis and intact hair follicles. (D.1 and D.2) Moderate

pathology (mouse #89) with diffuse inflammation, tissue damage and presence of AFB. (E1,E2) Necrosis, granuloma formation, inflammation and abundant extracellular clustering of AFB was observed in mice with severe pathology (mouse #84).

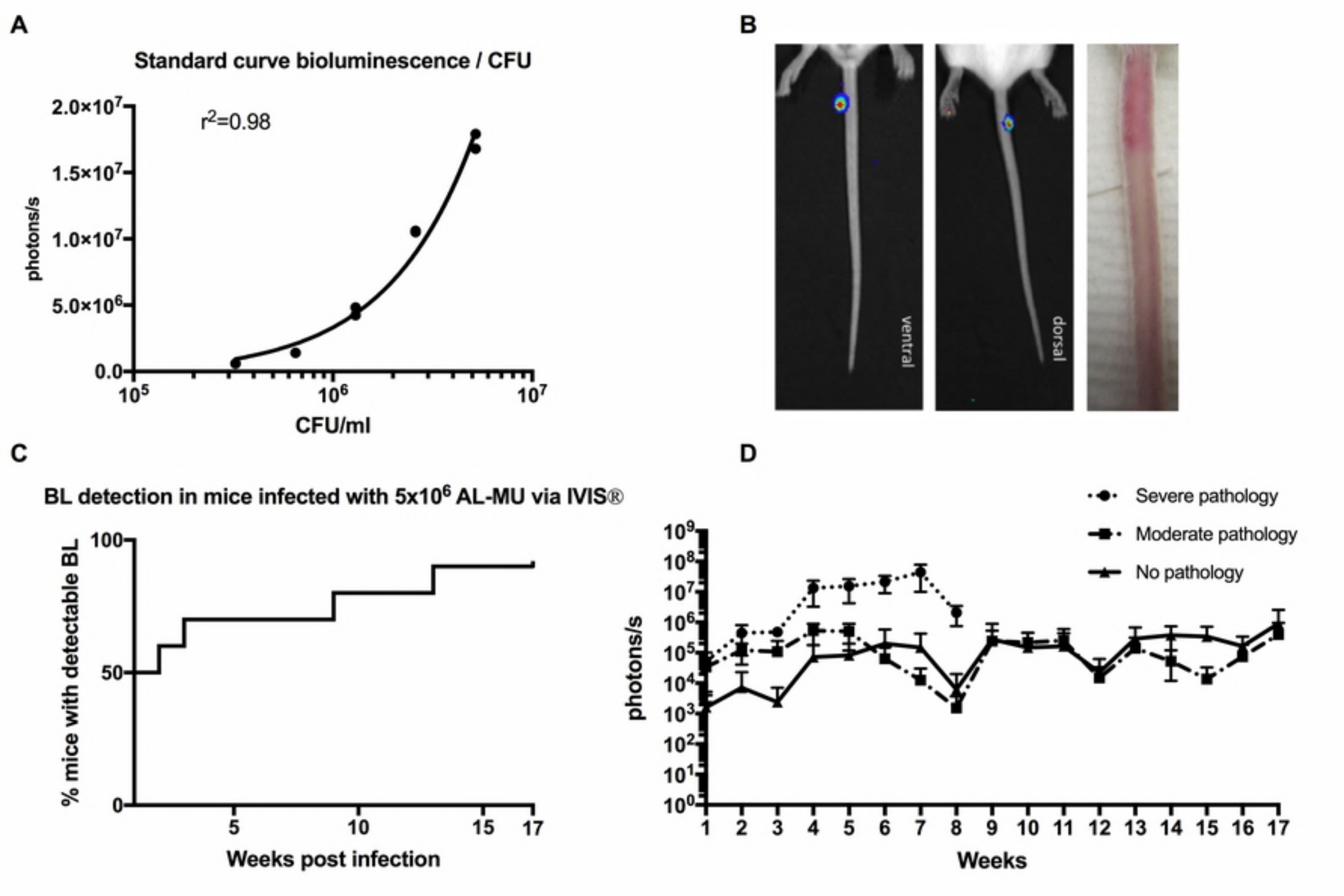
A
Standard curve bioluminescence / CFU
r2=0.98
2.0×10^7
1.5×10^7
1.0×10^7
5.0×10^6
0.0
photons/s
10^5
10^6
10^7
CFU/ml
B
ventral
dorsal
C
BL detection in mice infected with 5x10^6 AL-MU via IVIS®
% mice with detectable BL
100
50
0
5
10
15
17
Weeks post infection
D
Severe pathology
Moderate pathology
No pathology
photons/s
10^9
10^8
10^7
10^6
10^5
10^4
10^3
10^2
10^1
10^0
1 2 3 4 5 6 7 8 9 10 11 12 13 14 15 16 17
Weeks

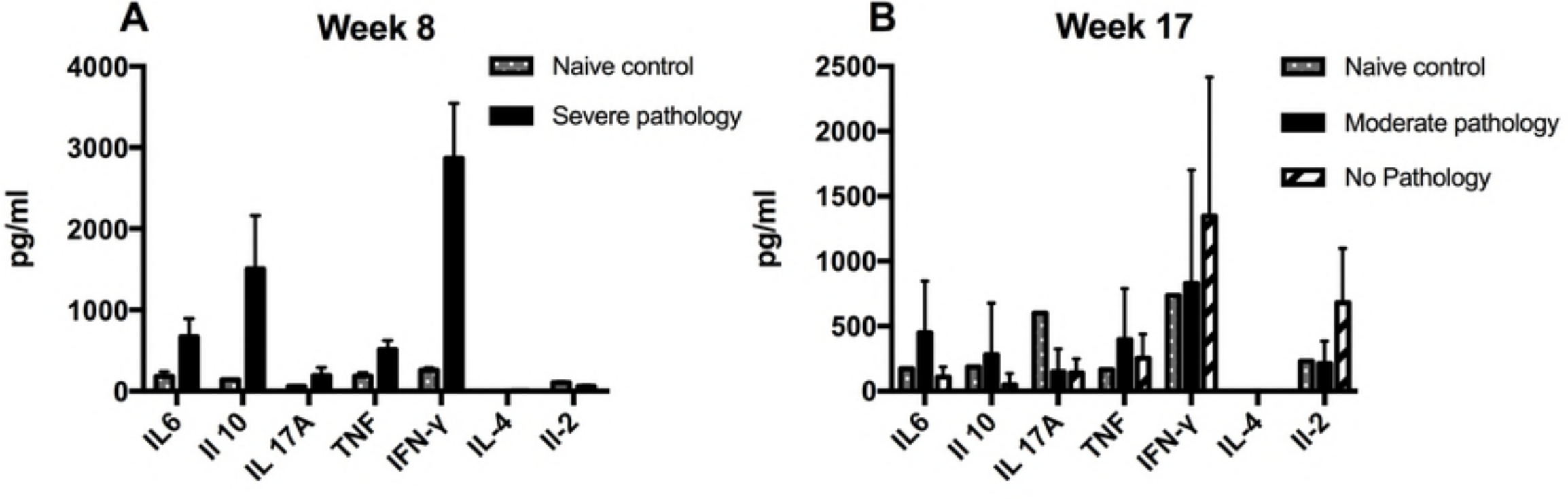
A
Week 8
Naive control
Severe pathology
pg/ml
4000
3000
2000
1000
0
IL6
Il 10
IL 17A
TNF
IFN-Y
IL-4
Il-2
B
Week 17
Naive control
Moderate pathology
No Pathology
pg/ml
2500
2000
1500
1000
500
0
IL6
Il 10
IL 17A
TNF
IFN-Y
IL-4
Il-2

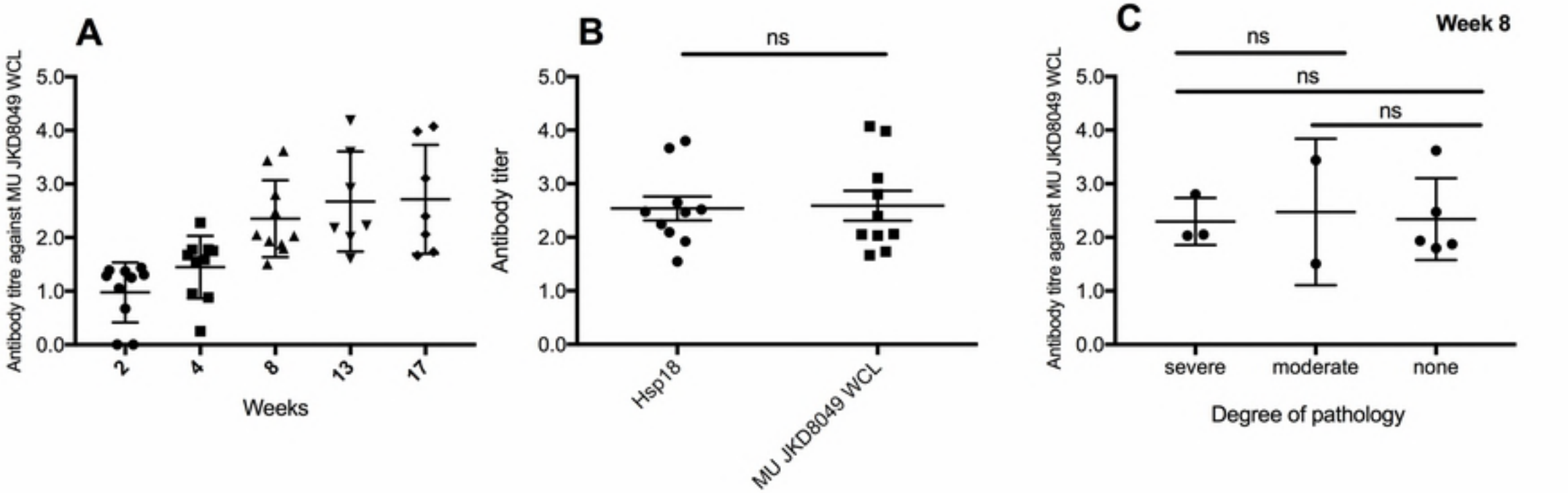
A
Antibody titre against MU JKD8049 WCL
5.0
4.0
3.0
2.0
1.0
0.0
2
4
8
13
17
Weeks
B
ns
Antibody titer
5.0
4.0
3.0
2.0
1.0
0.0
Hsp18
MU JKD8049 WCL
C
Week 8
ns
ns
ns
Antibody titre against MU JKD8049 WCL
5.0
4.0
3.0
2.0
1.0
0.0
severe
moderate
none
Degree of pathology